Recognition of Motor-Imagery Electroencephalography Using Fuzzy Clustering Neural Networks

[1,*] Chi-Yuan Lin and [2] Yi-Fang Chen

Abstract

In this paper, a motor-imagery electroencephalography recognition system is proposed on single-trial motor imagery (MI) data. The main purpose of this paper is to analyze the visualized left- and right-hand behavior when single-trial EEG signals are offline in a brain-computer interface application. The frequency band of EEG variations in Channels C3 and C4 of the research subjects is filtered using a Butterworth filter, and a filtered band is used to extract the average energy of the two channels and construct 2D feature vectors. This facilitated the identification and classification of left- and right-hand behavior using unsupervised fuzzy Hopfield neural network (FHNN) clustering. Compared with LDA and SVM from experimental results, FHNN clustering provides a potential for BCI application.

Keywords: single-trial motor imagery (MI), electroencephalography (EEG), Butterworth filter, fuzzy Hopfield neural network (FHNN)

1. Introduction

The brain–computer interface (BCI) is a communication system that provides an alternative channel for directly transmitting messages from the human brain to computers by analyzing the brain's mental activities [1–3]. BCI systems based on the single-trial analysis of electroencephalographic (EEG) signals associated with imagined finger movements (motor imagery; MI) have grown rapidly in the last decade [2].

As early as 1875, British physiologist Richard Carton measured weak brain signals by attaching electrodes to the scalp of monkeys and rabbits. He also discovered and clearly identified evoked potentials, and the voltage changes that occur in the brain, sensory organs, and neural pathways, facilitating the brain to respond to external stimuli [4].

Since the recording of human brain electroencephalograms (EEGs) by German psychiatrist Hans Berger in 1929, EEG research and application have achieved the following developments: (a) the origins of EEG signals (the basis of neurophysiology and cell biology); (b) EEG applications for clinical diagnosis and treatment; and (c) brain neuron cognition and brain interface applications. Dedicating several years to extensive research, Berger was the first to publish records of human EEG. Since then, EEG has been applied to the medical field. In this paper, only EEG signals of specific frequencies are used.

Supervised classifiers are usually applied to recognize MI EEG data in most BCI systems, such as linear discriminant analysis (LDA) [5] , which is quite popular and is generally used to classify what need to be discriminated. The fuzzy Hopfield neural network (FHNN) clustering is an unsupervised approach that partitions a collection of feature vectors into a number of subgroups based on minimizing the trace of a within-cluster scatter matrix. EEG data are non-stationary and their characteristics vary with time; therefore, the classification of MI EEG data with an unsupervised FHNN clustering may lead to a better classification accuracy than others that can be obtained with conventional supervised classifiers.

To assess the performance of FHNN clustering, we use some classifiers, such as LDA, and SVM, to classify the single-trial MI data, and the experiments also show that there is great potential for the use of unsupervised FHNN in EEG data classification.

This paper is organized as follows: In Section II, Background description is presented; Data collection and experiment procedures are presented in Section III; Classification and Recognition of the Time-Domain Features of Imaginary Movements are presented in Section IV; Results and discussions are presented in Section V. Finally, conclusions are given in Section VI.

*Corresponding Author: Chi-Yuan Lin
(E-mail: chiyuan@ncut.edu.tw)
[1, 2.] Department of Computer Science and Information Engineering, National Chin-Yi University of Technology,, No.57, Sec. 2, Zhongshan Rd., Taiping Dist., Taichung 41170, Taiwan

2. Background Description

EEG signals reflect the electrical activity of 100 billion neurons in the brain and are the bridge between neurons that trigger the transmission of adjacent neurons. On average, a neuron has 5,000 synapses. Because the electrical activity of one neuron is extremely minute, a modern EEG can only measure the electrical activity of a cluster of neuron [6].

EEG is the representation of electrical activity and contains four frequency bands depending on the wave number per unit of time. In 1908, EEG was used to recognize the α wave for the first time; subsequently, various types of EEG have been described to correspond to different mental states. Under normal circumstances, human brains exhibit a combination of several frequencies at any given time. One of these frequencies dominates the main EEG depending on the subject's state of consciousness.

Researchers endeavor to observe the EEG activity and mental state that allow people to consciously control their thoughts and orient EEG into an ideal state.

A conscious person may exhibit different EEG frequencies in various mental states. For example, a person that prepares to exercise shows weakened signal power at certain rhythms or frequencies. Figure 1 shows the four ranges of the EEG spectrum [7].

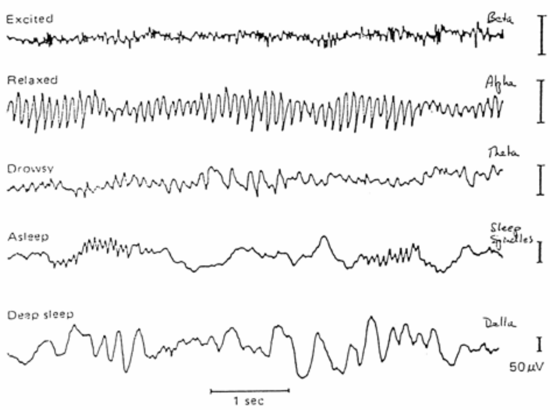

Figure 1: Basic background waves

α waves typically occur when a conscious person is at rest or closing his eyes. The highest amplitude of α waves (30–50 u V) is observed in the postcentral gyrus and occipital lobe.

β waves, also known as fast waves, are higher than 13 Hz in frequency, and possess an amplitude lower than 20 u V, which can be found in the postcentral gyrus, occipital lobe, and frontal lobe. Generally, u waves are mixed with α waves, and the extent to which differs from person to person. When people are in a stimulated state, such as their eyes being open or experiencing pain or tension, α waves are suppressed, and β waves increase.

θ and δ waves are also known as slow waves; θ waves exhibit a frequency of approximately 3 Hz, and δ waves range between 4 and 7 Hz. Slow waves generate comparatively higher amplitudes of up to hundreds of millivolts. These waves are commonly observed in the brains of children that are awake and adults that are sleeping.

2.1 Event-related Potential

Traditionally, an EEG is compiled by collecting EEG signals without stimulating the subject. Another method is to observe EEG variations after stimulating the subject. The latter method is employed to analyze specific related events and filter redundant noises for convenient observation using evoked potential or event-related potential (ERP). ERPs induce the time-locked variations of activated neurons. This technology has recently attracted increasing attention.

ERP technology enables researchers to use a raw EEG to record electrical activities in the brain and investigate the human cognition. For this purpose, subjects are instructed to perform predetermined missions that trigger the feedback of intended cognition (e.g., attaining goals of a certain type); subsequently, the EEGs of the subjects are recorded. Therefore, ERP is the potential variation in human responses to internal or external events.

A raw EEG records all electrical activities of a subject's brain at a given time (Figure 2). To extract messages of interest, time-locked and average signals must be identified by marking the time of stimuli and averaging the results of numerous experiments (Figure 3) [8].

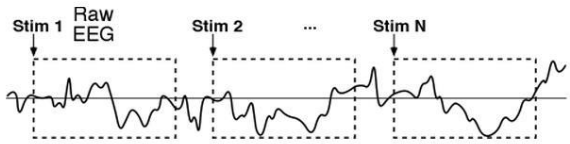

Figure 2: The sum of all electrical activity in the brain and the raw EEG signals of a subject during a specific period

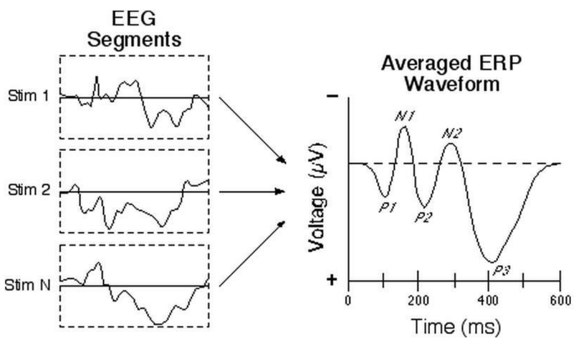

Figure 3: The averaged waveform of stimuli before 100 ms

This averaging procedure involves filtering stimuli unrelated to brain activities. Random variations are averaged, and sufficient experiments are conducted to isolate visual stimuli related to electrophysiological activities using ERP waveforms. The peak values of most waveforms are then linked to specific cognitive mechanisms. Because of the electrophysiological phenomenon, ERP shows a superior temporal resolution, but, comparatively, a smaller spatial resolution. Thus, ERP is a key tool for understanding cognitive procedures.

In 1977 and 1992, Gert Pfurtscheller proposed two phenomena, namely event-related desynchronization (ERD) and event-related synchronization (ERS). These phenomena were introduced to explain the potential electrical differences of an EEG, which are caused by internal or external stimuli. ERD reflects the energy suppression in the EEG that results from unsynchronized neurons. ERS reflects the energy increase caused by synchronized neurons [9].

2.2 Event-related Desynchronization and Event-related Synchronization

ERD is the amplitude attenuation of EEG alpha rhythms that occur in related events. Closely related to cerebral cortex activation and consciousness, ERD is associated not only with the electrophysiological procedures of cerebral cortex activation and stimulation, but also with sensory messages in the cerebral cortex and the characteristics of motor command execution. ERD has been studied using visual and audio stimuli, such as random motion, cognition, and attention missions. Numerous studies have adopted visual stimuli for experiments. In addition, ERD can reflect the difference in relative sensitivity during the process of memorization. Furthermore, ERD alpha waves show significant differences between the lower frequency band (8–10 Hz) and the higher frequency band (10–12 Hz). The components of these two alpha bands may reveal different cognitive processes.

Research has found that ERD alpha waves of the lower frequency (8–10 Hz) signify processes of attention and activation. The higher frequency band of ERD alpha waves (10–12 Hz) is related to more stimulating events. The counterpart mechanism of the ERD is the ERS, which can be observed when the alpha activity increases in particular stages or regions. ERS indicates whether the cerebral cortex is at rest or idle. ERS results represented by ERD mapping patterns can be used to investigate the time and phase of cortex activation models.

The ERD brain mapping technique can be used to illustrate abstract regions where the brain activity occurs with a higher temporal resolution. This feature is the reason why ERD is particularly appropriate for investigating cognitive processes. Because of the thriving development of computer technology, the ERP technique combined with audio stimuli has become a core element of experiments regarding human psychology and physiology. However, several studies have contended that ERD is not stable and not totally independent in the EEG. Recently, Klimesch suggested that ERD synchronous oscillations results from transiently phase-locked events or stimuli [10].

Synchronizing the frequency of the theta rhythm produces ERP because the frequency of the alpha rhythm is typically not synchronized with mission demands. Therefore, ERD alpha frequencies provide functional messages of various cortices for the ERP technique. This implies that ERD and ERS techniques can be adopted to identify ERPs that cannot be found by measuring event-related brain activities.

Additionally, with most BCI applications, ERD and ERS can be triggered by visualized motions rather than real motions. Therefore, since 1980, several BCIs based on α/β have been developed [11].

3. Data Collection and Experiment Procedures

The brain wave data used in this study are derived through off-line data analysis. The data source is the public information provided by a graduate institute of biomedical engineering at Graz University of Technology, Austria that was provided for the 2003 BCI Competition II [12]. The participant recorded in this data was a healthy 25 year-old female. The participant was placed in a comfortable armchair. Next, the corresponding hand movements that control the movement (to the left or right) of the image on the feedback column were shown to the participant. The prompts for moving the image to the left or right were randomly assigned.

The experiment conducted in this study involved 7 procedures comprising 40 tests (Figure 4). Each procedure was completed in one day. Intervals of several minutes were provided between tests. A total of 280 samples (140 from each class) were employed. Each test lasted for 9 s: The first two seconds were motionlessly followed by an audio stimulating instruction that indicated the start of the test. The trigger channel (#4) was switched from low to high, and the plus sign appeared for a second. At the 3rd second, an arrow pointing to either left or right appeared. Feedback was provided through Channels 1 (C3) and 3 (C4) (Fig. 5). The AAR parameters were integrated with discriminant analysis of the output parameters. The classification results obtained were provided to the participants as the feedback signals. EEG signals were measured using G-tec amplifiers and Ag/AgCl adhesive electrodes. Three pairs of electrodes were placed at three EEG channels (C3, Cz, and C4). Pads with the plus sign were attached at the front, and those with a minus sign were attached at the back.

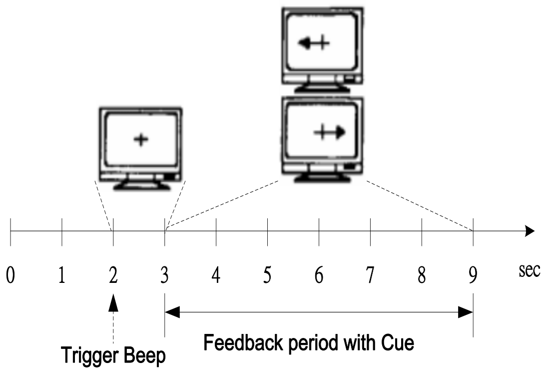

Figure 4: Experiment flowchart

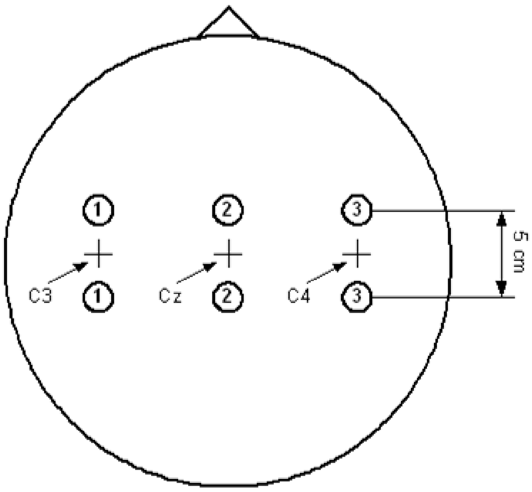

Figure 5: Electrode distribution

4. Recognition of the Time-domain Features of Imaginary Movements

4.1 Butterworth Filter

Butterworth filters were adopted to process EEG signals; these filters were bandpass filters with specific mu and beta wave frequencies. The central frequencies of the bandpass constant Q of the Butterworth filters were 6, 6.9, 7.8, 9, 10.2, 11.7, 13.4, 15.3, 17.5, 20.0, 22.8, 26.1, 29.8, and 33.5 Hz.

A set of 4th order Butterworth bandpass filters was constructed; these filters shared the same central frequencies for constant Q. The rule determining how these filters overlapped with adjacent filters was established based on the standard central frequency, which was the point next to the start frequency [13].

The Butterworth bandpass filters used in this paper had a 128 Hz sampling frequency. When the sampling frequency reaches the desired frequency (8–30 Hz, that is, the frequency band of mu and beta waves), the desired frequency can subsequently be extracted, as shown in Figs. 6 and 7.

4.2 Time-domain Feature

The EEG amplitude in the motor cortex decreased significantly when visualized actions were performed in response to the task signs. The ratio of the sum of C3 amplitudes to that of C4 amplitudes was regarded as the time-domain feature; thus, the most distinct ERD feature in the time domain was identified.

The results of the experiment conducted in this paper indicated that if time was segmented into durations of 1.5 s for the sequential analysis, the segment of 4–5.5 s provided satisfactory results.

According to the Figures 8 ~ 11, after noise was filtered, the signal amplitude stabilized, and the time-domain feature of ERD was more distinct.

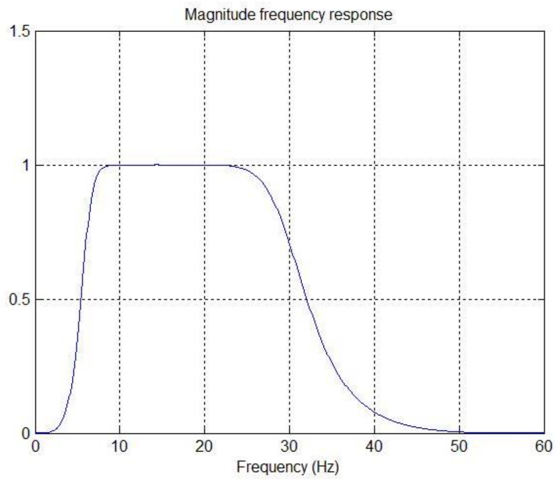

Figure 6: Frequency response curve

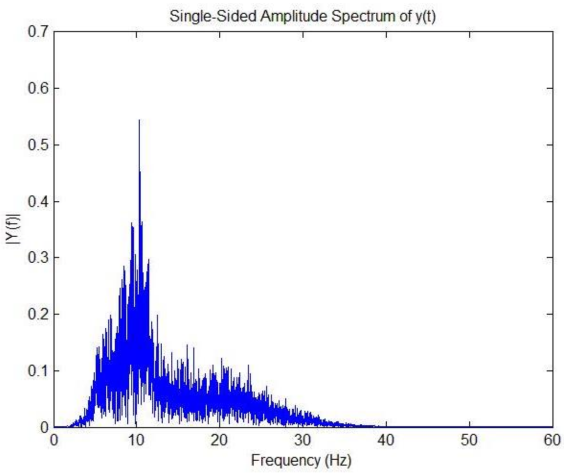

Figure 7: The amplitude of filtered raw signals

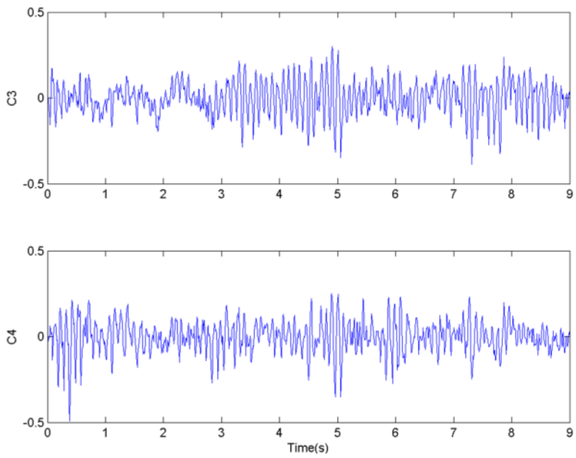

Figure 8: The raw EEG for left-hand visualized motions

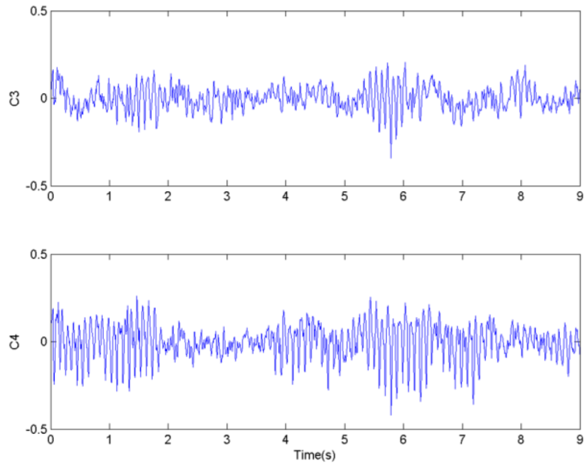

Figure 9: The raw EEG for right-hand visualized motions

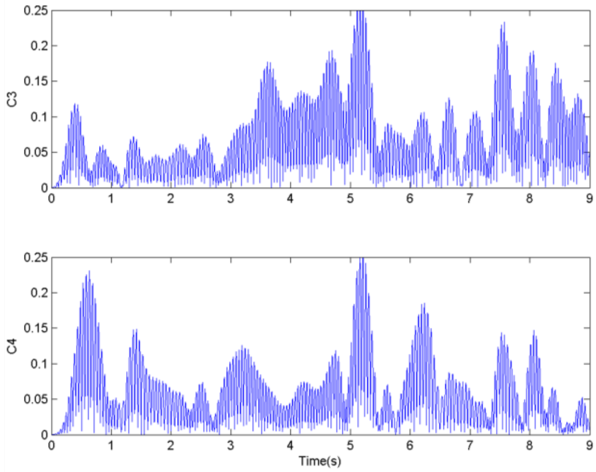

Figure 10: The EEG for left-hand visualized motions after noise was filtered using a Butterworth filter

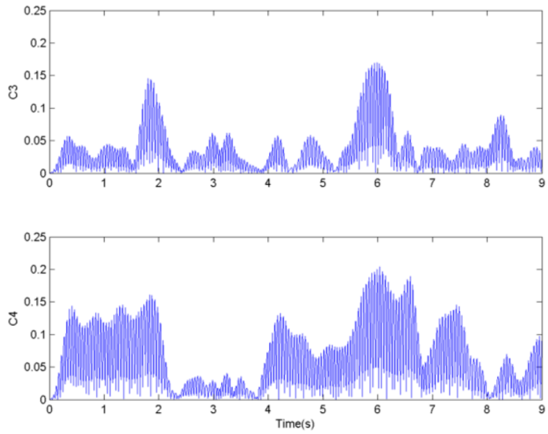

Figure 11: The EEG for right-hand visualized motions after noise was filtered using a Butterworth filter

4.3 Feature Extraction

Let f_t be the time-variant function of EEG amplitudes. The energy of the C3 and C4 channels in each test can be obtained using the time-domain energy calculation method.

$$E_{C3} = \sum_t \left| f(t)^q_{C3} \right|^2 \tag{1}$$

$$E_{C4} = \sum_t \left| f(t)^q_{C4} \right|^2 \tag{2}$$

During the task of visualized left-hand motions, Channel C3 (the cerebral sensorimotor region corresponding to the left hand) exhibited an energy increase, which matched the ERS characteristics. Channel C4 (the cerebral sensorimotor region corresponding to the right hand) exhibited an energy decrease, which matched the ERD characteristics. ERS and ERD were also observed during the task of visualized right-hand motions.

The feature of the i th test was obtained using

$$f^t = \left[mean\left(E^i_{C3}\right), mean\left(E^i_{C4}\right) \right] \tag{3}$$

The feature matrices of both the training data and test data were 140×2 .

4.4 Fuzzy Hopfield Neural Network Clustering Techniques

Clustering is a process for classifying training samples in such a way that samples within a cluster are more similar to each other than samples belonging to different clusters. Similarity measures employed to classify samples depend on the object characteristics e.g. distance, vector, entropy, etc. Many clustering approaches have also been demonstrated such as the hard clustering algorithm [14-15] and the soft (fuzzy) clustering algorithm.

Each of them has its own special characteristics. There have been many applications based on clustering strategy; some of these applications designed by authors include image segmentation [16] and fuzzy vector quantization algorithms [17]. The fuzzy clustering method assigns the sample with a number, m, between zero and one described as a membership function. In this paper, the fuzzy clustering method is to classify the feature vectors extracted from the original EEG data, and to recognize complicated brain mental tasks, such as left and right motor imageries.

The FCM clustering algorithm was first introduced by Dunn [18], and the related formulations and algorithms were extended by Bezdek [19]. Another strategy for fuzzy clustering, called the penalized fuzzy c-means (PFCM) algorithm, with the addition of a penalty term was proposed by Yang [20-21]. It is a generalized FCM algorithm and was shown by Yang that the PFCM algorithm is more meaningful and effective than the FCM. The Hopfield neural network with a simple architecture and parallel potential has been applied in many fields [17, 22-23]. By using Eqs. (4) and (5),

$$Net_{i,j} = \left\| \mathbf{x}_i - \sum_{k=1}^{n} \frac{1}{\sum_{h=1}^{n} \left(u_{h,j}\right)^m} x_k \left(u_{k,j}\right)^m \right\|^2 \tag{4}$$

$$u_{i,j} = \left[\sum_{\ell=1}^{c} \left(\frac{Net_{i,j}}{Net_{i,\ell}} \right)^{1/m-1} \right]^{-1}, \textit{for all } j \tag{5}$$

the FHNN can classify training samples into c classes in a parallel manner that is described as follows:

FHNN Clustering Algorithm

Step 1. Input a set of training samples $X = \{x_1, x_2, \ldots, x_n\}$, constant v $(v > 0)$, fuzzification parameter m $(1 \le m < \infty)$, the number of class c, and initialize the states for all neurons $U = [u_{i,j}]$ (membership matrix).

Step 2. Compute α_j and weighted matrix using Eqs.

$$\alpha_j = \frac{\sum_{i=1}^{n} u_{i,j}^m}{\sum_{j=1}^{c}\sum_{i=1}^{n} u_{i,j}^m}, \; j = 1,2,\ldots,c,$$

and

$$W_{i,j;k,j} = \frac{1}{\sum_{h=1}^{n} \left(u_{h,j}\right)^m} x_k \quad \text{, respectively.}$$

Step 3. Calculate the input to each neuron (i, j) by Eq. (4) .

Step 4. Apply Eq. (5) to update the neurons' membership values in a synchronous manner.

Step 5. Compute $\Delta = \max\left(\left\|U^{(t+1)} - U^{(t)}\right\|\right)$. If $\Delta > \varepsilon$ go to step 2, otherwise go to Step 6.

Step 6. Find the cluster for the final membership matrix.

5. Results and Discussions

This paper experimented on two sets of extracted features. Feature 1: The time domain was set as the feature vector and then classified using the LDA. Feature 2: ERD energy variations were classified using the FHNN. After these two features were extracted, the results were compared with the features extracted using the FHNN, and SVM.

Figs. 12 to 14 show the feature recognition results obtained using different classifiers. Both the LDA and SVM were supervised learning linear classifiers that can directly distinguish between the left and right hands. In addition, the FHNN adopted in this paper as an unsupervised algorithm did not require any training before the events to recognize left- and right-hand visualized motions. According to Figure 14, the FHNN only classified the results into two groups.

According to Feature 2 and Figure 15, during left-hand motion tasks, Channel C2 exhibited increased energy amplitudes corresponding to ERS characteristics, whereas channel C4 exhibited reduced energy amplitudes corresponding to ERD characteristics. Similarly, ERD and ERS were also observed during right-hand tasks (Fig. 16).

Figure 17 shows the 2 feature recognition results obtained using FHNN classifiers. Table 1 shows the recognition results for the two features. Both feature vectors performed two classification activities, that is, "determining whether the right-hand fingers moved" and "determining whether the left-hand fingers moved".

Furthermore, because the participants began their visualized motion tasks on the 3rd second, this paper observed information of the offline events during the analysis of time segment selection.

Classification performance were compared with that of the LDA. For segments 3s-9s, 3s-8s, 3s-7s, 3s-6s, and 3s-5s, the accuracy declined after 3s-9s, 3s-8s, and 3s-7s. Accordingly, this paper analyzed other time segments and found that 4s-6.5s was the segment that resulted in the greatest accuracy when using the SVM.

Although the FHNN demonstrated high recognition rates when classifying a specific period of time (3s-9s and 3.5s-9s), its performance in other time segments was lower than the LDA and SVM.

Therefore, based on practicality, the FHNN can be adopted for online classification because its recognition rates for periods of time are satisfactory. Additionally, the first 0.5s in the 3.5s-9s segment was the preparation time for the experiment participants.

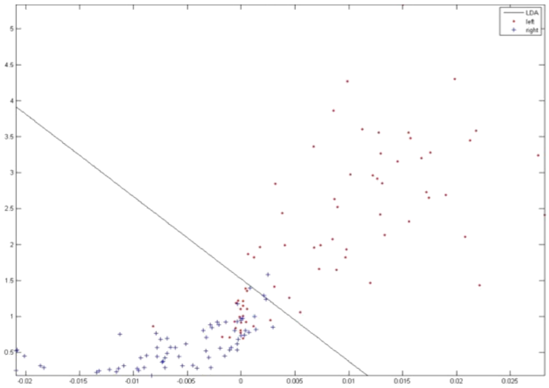

Figure 12: Classification result of the LDA

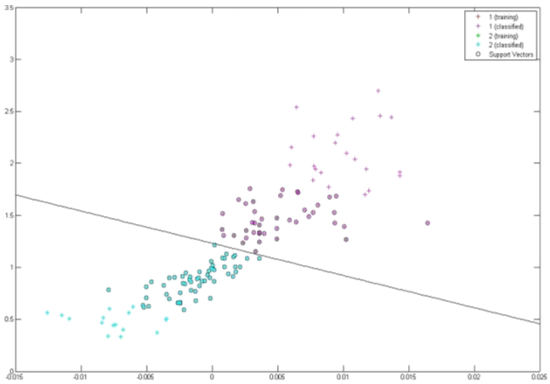

Figure 13: Classification result of the SVM

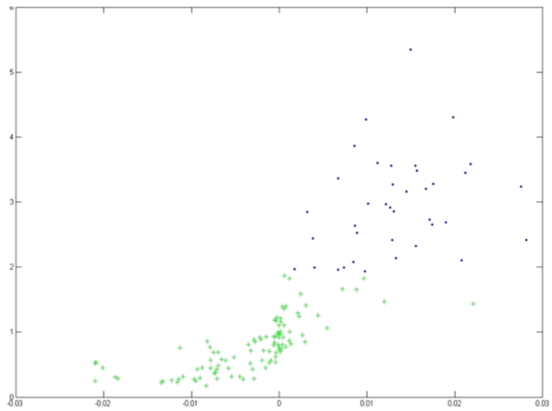

Figure 14: Classification result of the FHNN

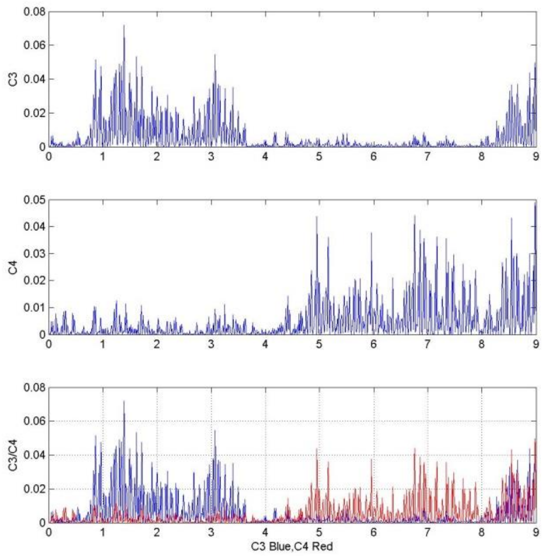

Figure 15: Variations in the energy amplitude of C3 and C4 during visualized left-hand motion tasks

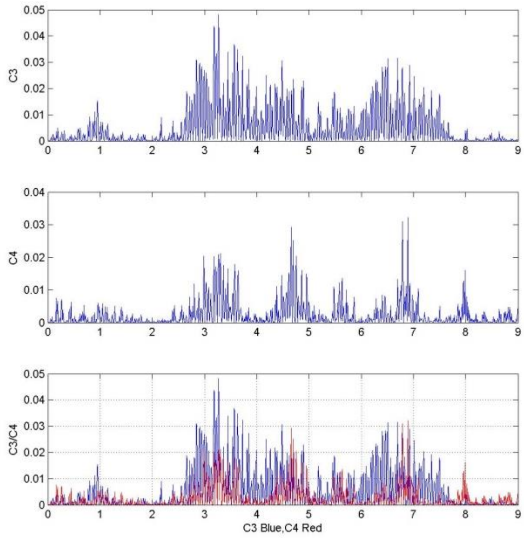

Figure 16: Variations in the energy amplitude of C3 and C4 during visualized right-hand motion tasks

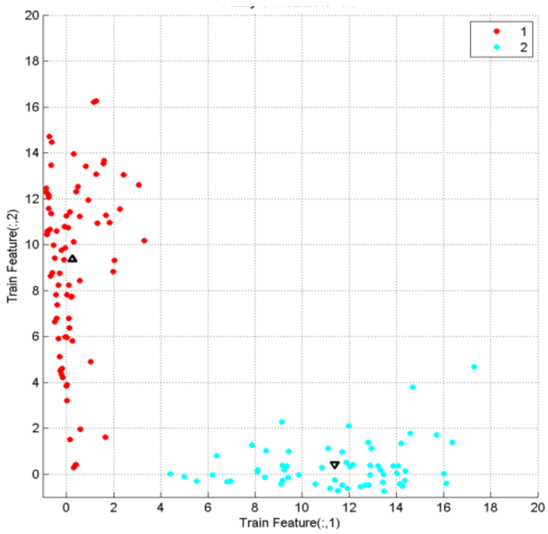

Figure 17: the recognition results for the two features

Table 1: Accuracy of time segment selection using various classifiers

Time segment selection	Accuracy		
	LDA	SVM	FHNN
3s-9s	77.86%	80.00%	**80.72%**
3s-8s	82.86%	82.14%	79.31%
3s-7s	82.14%	83.57%	80.01%
3s-6s	77.86%	76.43%	72.87%
3s-5s	71.43%	70.71%	66.45%
4s-9s	79.29%	80.71%	81.43%
5s-9s	72.14%	73.57%	74.31%
6s-9s	65.71%	67.14%	58.56%
7s-9s	60.00%	60.00%	59.33%
4s-6s	83.57%	86.43%	74.30%
4s-7s	84.29%	85.00%	80.70%
4s-8s	82.86%	83.57%	80.01%
4s-6.5s	85.00%	87.14%	76.43%
4s-7.5s	82.86%	83.57%	81.41%
3.5s-9s	79.29%	81.43%	**82.85%**
4.5s-9s	77.14%	80.71%	**78.58%**

Acknowledgments

The work was partially supported by the National Science Council of Taiwan, Republic of China under research contract NSC- 99-2221- E-167- 024 and NSC- 100-2221- E- 167- 024.

6. Conclusion

The objective of this paper was to increase the recognition rate of EEG applications based on BCIs. This paper extracted information of interest from the frequency and time domains before identifying and classifying the data. The desired frequencies were extracted using Butterworth filters for subsequent feature extraction, classification, and recognition. However, the EEG signals observed during performing the visualized tasks were generally weaker than those observed during performing the real motion tasks. In addition, the signals of interest were often hidden in continuous and irregular signals and noises. To resolve these issues, this paper performed several procedures to extract the desired features. Time-domain features were adopted for feature extraction. The methods of time segment selection were also classified. Based on the procedures of time segment selection, activity segment locations were specified, so classification accuracy was increased. Finally, the experimental results show that FHNN clustering is a promising approach showing splendid potential applications in BCI work.

References

[1]. Jd. R. Millán, F. Renkens, J. Mouriñ, W. Gerstner, “Noninvasive brain-actuated control of a mobile ro-bot by human EEG,” IEEE Trans. Biomed. Eng. 51 (6), pp. 1026–1033, 2004.

[2]. L. Parra, C. Alvino, A. C. Tang, B. A. Pearlmutter, N. Yeung, A. Osman, P. Sajda, “Linear spatial inte-gration for single trial detection in encephalography,” NeuroImage 7 (1), pp. 223–230, 2002.

[3]. J. R. Wolpaw, N. Birbaumer, D.J. McFarland, G. Pfurtscheller, T. M. Vaughan, “Brain-computer in-terfaces for communication and control,” Clin. Neu-rophysiol. 113, pp. 767–791, 2002.

[4]. A. Zaher, “Visual and Brainstem Auditory Evoked Potentials in Neurology,” EMG Methods for Evaluating Muscle and Nerve Function, PP.281-310, Jan. 2012.

[5]. R. Scherer, G. R. Muller, C. Neuper, B. Graimann, G. Pfurtscheller, “An asynchronously controlled EEG-based virtual keyboard: improvement of the spelling rate,” IEEE Trans. Biomed. Eng. 51, 979–984, 2004.

[6]. G. Pfurtscheller and C. Neuper, “Motor Imagery and Direct Brain-Computer Communication,” *Proc IEEE*, Vol. 89, No. 7, pp. 1123-1134, 2001.

[7]. Quantitative EEG - The NeuroDevelopment Cente(2013), “qEEG or quantitative EEG brain maps: see the reason for your struggles, then change it, ” [online]. vailable: http://neurodevelopmentcenter.com/neurofeedback-2/qeeg/

[8]. Makeig S, Westerfield M, Jung T P, et al, "Dynamic brain sources of visual evoked responses." *Science* , Vol.295, pp. 690-694, 2002.

[9]. G. Pfurtscheller, F. H. Lopes and Sulva da, "Event-related EEG/MEG synchronization and desynchronization: basic principles," *Electroencephalogr. Clin. Neurophysiol*., Vol. 100, pp. 1842-1857, 1999.

[10]. Krause, C. M., Lang, A. H., Laine, M., Kuusisto, M., and Porn, B. "Event-related EEG desynchronization and synchronization during an auditory memory task," *Electroencephalography and Clinical* Neurophysiology, Vol. 89, NO. (4), pp. 319-326, 1996.

[11]. J.R. Wolpaw, D.J. McFarland, "EEG-based brain–computer communication," Electroencephalogr. Clin. Neurophysiol., vol. 90, pp. 444 - 449, 1994.

[12]. BCI Competition III (2003) [online], vailable: http://www.bbci.de/competition/iii/.

[13]. T. Wang, et al." Classifying EEG-based motor imagery tasks by means of time-frequency synthesized spatial patterns," Clin. Neurophysiol. 115, pp. 2744–2753, 2004.

[14]. L. Bobrowski and J. C. Bezdek, "C-means cluster-ing with the and norms," IEEE Trans. Syst. Man. Cybern., vol. 21, pp. 545-554. 1991.

[15]. P. Y. Yin and L. H. Chen, "A new non-iterative approach for clustering," Pattern Recognition Lett., vol. 15, pp.125-133, 1994.

[16]. W. F. Kuo, C. Y. Lin, and Y. N. Sun, "Brain MR Images Segmentation Using Statistical Ratio: Map-ping between Watershed and Competitive Hopfield Clustering Network Algorithms", Computer Methods and Programs in Biomedicine,Vol. 91, No. 3, pp. 191-198, Sep. 2008.

[17]. C. Y. Lin and C. H. Chen, "An Invisible Hybrid Color Image System Using Spread Vector Quantiza-tion Neural Networks with Penalized FCM," Pattern Recognition, Vol. 40, No. 6, pp. 1685-1694, June 2007.

[18]. J. C. Dunn, "A fuzzy Relative of the ISODATA process and its use in detecting compact well-separated clusters," J. Cybern., vol.3, no3, pp.32-57,1974.

[19]. J. C. Bezdek, "Fuzzy mathematics in Pattern Classification," Ph.D. Dissertation, Applied Mathematics. Cornell University, Ithaca, New York, 1973.

[20]. M. S. Yang, "On a class of fuzzy classification maximum likehood procedures," Fuzzy Sets and Systems 57, 365, 1993.

[21]. M. S. Yang, and C. F. Su, "On parameter estimation for normal mixtures based on fuzzy clustering algorithms," Fuzzy sets and Systems, 68, 13, 1994.

[22]. K. S. Cheng, J. S. Lin, and C. W. Mao, "The appli-cation of competitive Hopfield neural network to medical image segmentation," IEEE Trans. med. Imaging, Vol. 15, pp. 560-567, 1996.

[23]. P. C. Chung, C. T. Tsai, E. L. Chen, and Y. N. Sun, "Polygonal approximation using a competitive Hop-field neural network," Pattern Recognition, Vol. 27, pp. 1505-1512, 1994.

Chi-Yuan Lin received the B.S. degree in Electronic Engineering from National Taiwan University of Science and Technology, Taiwan, in 1988, the M.S. degree in Electronic and Information Engineering from National Yunlin University of Science and Technology, Taiwan, in 1998, and the Ph.D. degree in Electrical Engineering from National Cheng Kung University, Taiwan, in 2004. Since 1983, he has been with the Department of Electronic Engineering at National Chin-Yi University of Technology in Taiwan where he is now a professor. His research interests include neural networks, multimedia coding, and signal processing.

Yi-Fang Chen received the B.S. degree in Electronic Engineering from National Chin-Yi University of Technology, Taiwan, in 2011, the M.S. degrees in Computer Science and Information from National Chin-Yi University of Technology, Taiwan, in 2013, His research interests include multimedia signal procession.